

# First Principle Simulations of Electronic and Optical Properties of a Hydrogen Terminated Diamond Doped by a Molybdenum Oxide Molecule

Joseph McGhee, Vihar P. Georgiev,

Device Modelling Group  
James Watt School of Engineering  
University of Glasgow, Glasgow G12 8QQ, United Kingdom  
E-mail: [vihar.georgiev@glasgow.ac.uk](mailto:vihar.georgiev@glasgow.ac.uk)

## ABSTRACT

In this work we investigate the surface transfer doping process induced between a hydrogen-terminated (100) diamond and a metal oxide  $\text{MoO}_3$ , using the Density Functional Theory (DFT) method. DFT allows us to calculate the electronic and optical properties of the hydrogen-terminated diamond (H-diamond) and establish a link between the underlying electronic structure and the charge transfer between the oxide materials and the H-diamond. Our results show that the metal oxide molecule can be described as an electron acceptor and extracts the electrons from the diamond creating 2D hole gas in the diamond surface. Hence, this metal oxide molecule acts as a p-type doping material for the diamond.

## INTRODUCTION

Diamond is a compound semiconductor material with many electronic applications such as microwave electronic devices [1], bipolar junction transistors [2] and Schottky diodes [3]. However, one of the most promising areas for diamond industrial application is in high-performance field effect transistors (FETs) used in the production of high frequency and high-power electronic devices [4]. Its properties potentially enable devices that are beyond the scope of current systems in terms of operating frequency, power handling capacity, operating voltage, thermal robustness and operating environment. This is due to the fact that diamond has a wide band-gap of 5.5eV, a thermal conductivity 5 times greater than 4H-SiC of 24 W/cm<sup>2</sup>\*K (for CVD diamond), a high breakdown field of 20Wcm<sup>-1</sup> and high hole and electron carrier velocities of 0.8x10<sup>7</sup>cm/s and 2.0x10<sup>7</sup>cm/s respectively. As a result, diamond is a superior new candidate for high frequency and high-power device applications [5].

However, the primary issue that has inhibited the application of diamond is the lack of a suitably efficient and stable doping mechanism. The most promising way to dope diamond is by surface transfer doping (STD), which is achieved by depositing different materials on the surface of diamond. For example, organic molecules, such as C<sub>60</sub> [6] and C<sub>60</sub>F<sub>48</sub> [7], can be used

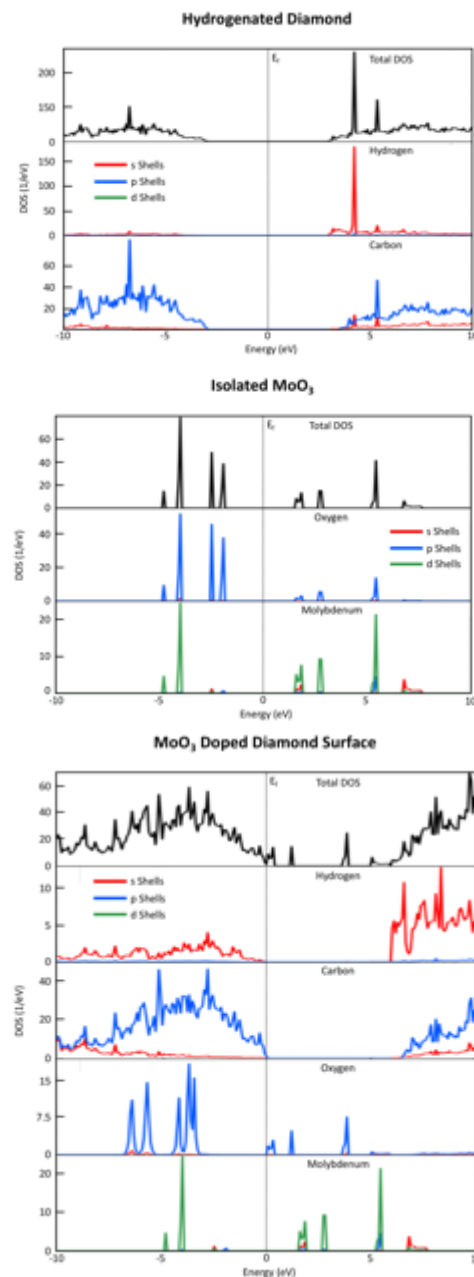


Figure 1. Top) Hydrogen terminated (100) diamond Density of States (DOS); Middle)  $\text{MoO}_3$  molecules DOS; Bottom)  $\text{MoO}_3$  molecule on the top of an H-Diamond.

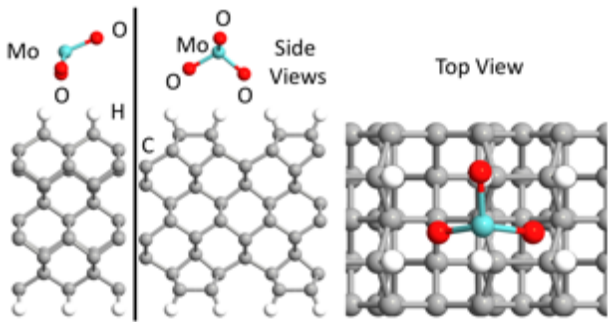


Figure 2. Simulated systems. The (left hand side) side view and (right hand side) top view of charge density different for the most stable  $\text{MoO}_3$ -doped diamond surface.

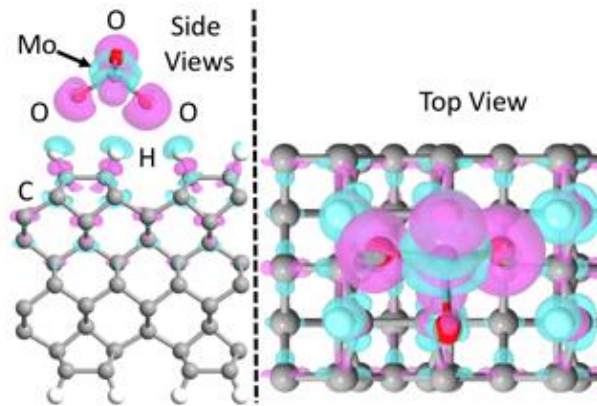


Figure 3. The (left hand side) side view and (right hand side) top view of charge density different for the most stable  $\text{MoO}_3$ -doped diamond surface. The purple regions represent electron accumulation and the green regions represent electron depletion (hole accumulation). The isosurface values are  $\pm 0.001 \text{ Bohr}^{-3}$ .

to deposit on the diamond surface and they will act as surface acceptors to induce holes in hydrogen terminated diamond (H-diamond). However, the organic molecules are not very stable in high temperatures and they are not compatible with the fabrication process. Hence, an alternative approach is to use inorganic components for STD, such as chromium oxide ( $\text{CrO}_3$ ) [8], molybdenum oxide ( $\text{MoO}_3$ ) [9, 10] and vanadium oxide ( $\text{V}_2\text{O}_5$ ) [11, 12].

In this paper, we would like to explore further than the previous research and explain in detail the process of STD of metal oxide materials, such as molybdenum oxide ( $\text{MoO}_3$ ), as a material for achieving such STD in diamond. In order to achieve our aim, we have performed numerical first principle simulations based on the Density Functional Theory (DFT).

### SIMULATION METHODOLOGY

All calculations were carried out using the Quantumwise Atomistix ToolKit (ATK) software using the DFT method [13]. The Generalised Gradient Approximation (GGA) exchange correlation was used for the geometry optimisations of the system and to obtain the total energies of the interfaced systems and the individual component parts, i.e. H-diamond and the oxide layer in question. For all geometry optimisations a force

tolerance of  $0.01 \text{ eV}/\text{\AA}$  was used. GGA-1/2 exchange correlation was used for all electronic structure calculations. To obtain a more accurate electronic description of the systems, DFT-1/2 method was used [14]. DFT-1/2 method is a semi-empirical approach that can overcome the error that local and semi-local exchange correlation density functionals inherently have when working with semiconductors and insulators. It works by correcting the self-interaction error of DFT by cancelling out the electron-hole self-interaction energy by defining an atomic self-energy potential. However, DFT-1/2 method is not suitable for calculating total energies, hence, we used GGA for the geometry optimisations and calculating adsorption energies. The Perdew, Burke and Ernzerhof (PBE) functional was chosen for all calculations because of the good match with experimental data (around 5.5 eV) regarding the value on the band gap in bulk diamond [11].

A Monkhorst-Pack scheme with an  $8 \times 8 \times 1$  k-point density ( $\text{\AA}$ ) mesh was used for the Brillouin zone integration. An iteration control tolerance of 0.0001 with a density cut off of  $1 \times 10^{-6}$  was used for all calculations with a medium basis set. The number of pseudo-atomic orbitals in a medium basis set is typically comparable to that of a double-zeta polarized (DZP) basis set [15]. The pseudopotential is SG15 and the density mesh cut-off is 185Ha, which gives a high accuracy with a medium computational efficiency.

### RESULTS AND DISCUSSION

Fig. 1 shows the total Density of States (DOS) and the partial DOS (PDOS) of a hydrogen terminated (100) diamond, the DOS of a single  $\text{MoO}_3$  molecule and the DOS of a  $\text{MoO}_3$ -doped H-diamond obtained from the DFT simulations. The PDOS gives us the possibility to separate the contribution of each atom in the overall profile of the full DOS of the materials. Also, the PDOS provides information about the different electronic shells of each element involved in the simulations. For example, when a diamond is hydrogen terminated the band gap is 5.9 eV (please see the top plot in Fig. 1). This is very close to the experimental value of 5.5 eV. Also, PDOS shows that the conduction band is mainly determined by the carbon p-shells. This is exactly what is expected because the carbon is a p-type element with valence electrons occupying  $p_x$ ,  $p_y$  and  $p_z$  atomic orbitals. The same plot reveals that the conduction band is mainly formed by the hydrogen atoms with electrons in the s-shell. Indeed, each H atom has  $1s_1$  electronic configuration that makes H an s-type element.

Following the discussion above, it can be concluded that the  $\text{MoO}_3$  molecule has a band gap of around 2.5 eV. This again is comparable to the reported experimental values of 3.2 eV and 2.8 eV for bulk and polycrystalline  $\text{MoO}_3$ , respectively,

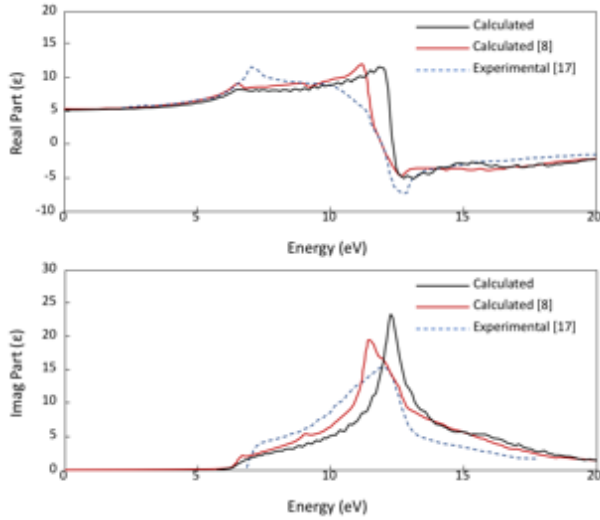


Figure 4. Dielectric constant plots for a bulk diamond comparing our calculated results with calculated results by Xiang *et al.* [8] and experimental results by Philipp and Taft [17].

obtained by the absorption spectra measurements [16]. The PDOS plots in Fig. 1 show that the oxygen p-shells are dominant in the valence bands while the d-shell (states) of the metal atoms are localised both in the conduction and the valence band. The Mo atom is a d-element and hence only the d-shells are visible in the PDOS and active in the chemical reaction.

The bottom part of Fig. 1 shows the DOS and the PDOS diagram for MoO<sub>3</sub> adsorbed on the H-diamond surface. There is a shift of the DOS to higher energies and the Fermi Level ( $E_F$ ) is in contact with the valence states. Moreover, the band gap of the diamond remains constant but states of the Valance Band Maximum (VBM) have crossed the Fermi Level, which in turn means that charge transfer has occurred as previously occupied states within the H-diamond are now vacant. This demonstrates that electrons have transferred from the diamond surface to the MoO<sub>3</sub> molecule leaving the hole accumulation layers. Moreover, this transfer of electrons can be directly linked with exchange of charge between the oxygen atoms from the MoO<sub>3</sub> molecule and the carbon hydrogen atoms of the H-diamond. The PDOS for the Mo atoms is virtually not modified in comparison to the isolated molecule presented in Fig. 1.

Fig. 2 shows the atomic position of the simulated MoO<sub>3</sub>:H-diamond interface. This configuration has the lowest energy in comparison to the other twelve systems of varying MoO<sub>3</sub> positions and orientations that we simulated. Hence, we used this system for further analysis.

Fig. 3 shows the electron density change for the most energetically stable MoO<sub>3</sub>:H-diamond interface. The blue regions show where there is a loss of electron density and thus the accumulations of holes, and the purple regions show where there is an increase in electron density. Hence, there is a hole

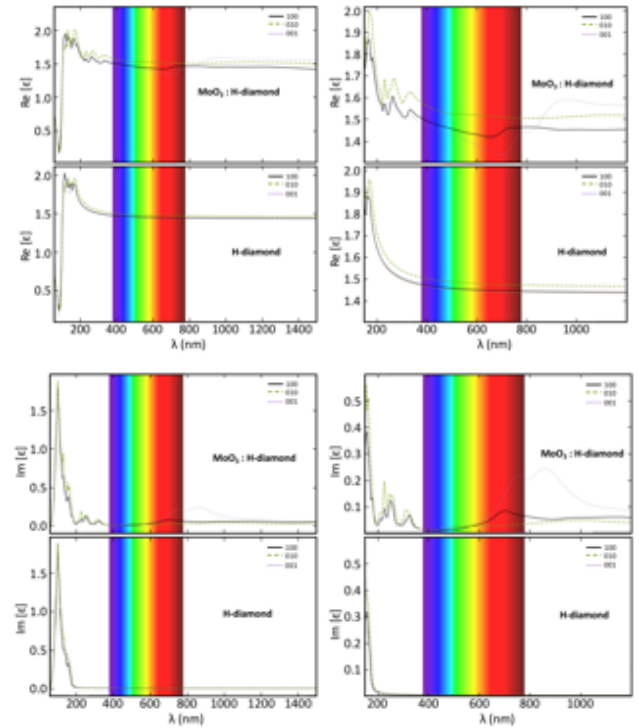


Figure 5. The dielectric function of the real ( $\text{Re}[\epsilon]$ ) and imaginary ( $\text{Im}[\epsilon]$ ) parts for the clean hydrogenated diamond surface and the most preferred MoO<sub>3</sub>-doped diamond surface. The results are superimposed of the visible spectrum.

accumulation that occurs near the surface of the diamond while most of the electron density gained by the MoO<sub>3</sub> clearly migrates to the O atoms. Therefore, the MoO<sub>3</sub> acts as a p-type doping material. This indeed is in agreement with the discussions above and the data presented in Fig. 1.

To further validate the reliability of our calculation parameters, we calculated the optical spectrum of a bulk diamond and plotted the dielectric constant to compare our results to a recent theoretical study by Xiang *et al.* [8] and experimental data published by Philipp and Taft [17].

The comparison plots for the real ( $\text{Re}[\epsilon]$ ) and imaginary ( $\text{Im}[\epsilon]$ ) parts of the dielectric constant in Fig. 4 show that our DFT method produces results in agreement with other published theoretical work and experimental data. For the bulk diamond, the spectrums of [100, 010, 001] crystallography orientation are degenerate and hence only one result for [100] orientation is presented. The small discrepancies between the calculated and the experimental curves are due to the inter-band transitions and neglected excitonic effects in the simulations. It should be pointed out that the absorption edge corresponding to the bulk gap of diamond of 5.5 eV is suppressed in the experimental spectre due to its indirect transition nature.

Fig. 5 shows the calculated real ( $\text{Re}[\epsilon]$ ) and the imaginary ( $\text{Im}[\epsilon]$ ) parts of the dielectric function of the type H-diamond and the MoO<sub>3</sub>:H-diamond system. For the pure H-diamond systems the spectra of [100, 010, 001] diamond crystallography

orientations are degenerate due to inherent structural anisotropy. However, this is not the case for the MoO<sub>3</sub>:H-diamond [100, 010, 001] surfaces. Depending on the substrate orientation, there is a significant difference in the visible part of spectrum. Also, the most significant difference between the pure diamond and the MoO<sub>3</sub>:H-diamond systems is at below 400 nm, where, due to the MoO<sub>3</sub> molecule, there are additional absorption features. Hence, this shows that the adsorption of the MoO<sub>3</sub> molecule on the H-diamond surface introduces new empty states within the diamond band gap that enhances the optical absorption of the MoO<sub>3</sub>-doped H-diamond near the infrared (IR) region.

## CONCLUSION

In this work we have performed the DFT simulations of a single molecule absorbed on a hydrogen terminated diamond substrate. The PDOS data shows that there is charge transfer between the MoO<sub>3</sub> molecule and the H-diamond. This is also confirmed by the charge density difference data. Hence, our results suggest that the MoO<sub>3</sub> molecule acts as a p-type doping material to the H-diamond surface.

Moreover, our optical simulation suggests that the MoO<sub>3</sub>-doped H-diamond may have great potential in application of opto-electronic devices for IR and near IR light detection. This is due to the fact that the MoO<sub>3</sub>-doped H-diamond systems have well pronounced peaks below the wavelength of the visible spectrum in the near IR wave lengths.

## REFERENCES

1. R.J. Trew, J. Yan and P.M. Mock, "The potential of diamond and SiC electronic devices for microwave and millimeter-wave power applications," *Proceedings of the IEEE*, vol. 79, no. 5, 1991, pp. 598-620; DOI 10.1109/5.90128.
2. M. Willander, M. Friesel, Q.-u. Wahab and B. Straumal, "Silicon carbide and diamond for high temperature device applications," *Journal of Materials Science: Materials in Electronics*, vol. 17, no. 1, 2006, pp. 1; DOI 10.1007/s10854-005-5137-4.
3. C. Wort and R. Balmer, "Diamond as an Electronic material," *Materials Today*, vol. 11, no. 1, 2008.
4. J. Liu, H. Ohsato, X. Wang, M. Liao and Y. Koide, "Design and fabrication of high-performance diamond triple-gate field-effect transistors," *Scientific Reports*, vol. 6, no. 1, 2016, pp. 34757; DOI 10.1038/srep34757.
5. S. Russell, S. Sharabi, A. Tallaire and D.A.J. Moran, "RF Operation of Hydrogen-Terminated Diamond Field Effect Transistors: A Comparative Study," *IEEE Transactions on Electron Devices*, vol. 62, no. 3, 2015, pp. 751-756; DOI 10.1109/TED.2015.2392798.
6. P. Strobel, M. Riedel, J. Ristein, L. Ley and O. Boltalina, "Surface transfer doping of diamond by fullerene," *Diamond and Related Materials*, vol. 14, no. 3, 2005, pp. 451-458; DOI <https://doi.org/10.1016/j.diamond.2004.12.051>.
7. M.T. Edmonds, M. Wanke, A. Tadich, H.M. Vulling, K.J. Rietwyk, P.L. Sharp, C.B. Stark, Y. Smets, A. Schenk, Q.H. Wu, L. Ley and C.I. Pakes, "Surface transfer doping of hydrogen-terminated diamond by C60F48: Energy level scheme and doping efficiency," *The Journal of Chemical Physics*, vol. 136, no. 12, 2012, pp. 124701; DOI 10.1063/1.3695643.
8. Y. Xiang, M. Jiang, H. Xiao, K. Xing, X. Peng, S. Zhang and D.-C. Qi, "A DFT study of the surface charge transfer doping of diamond by chromium trioxide," *Applied Surface Science*, vol. 496, 2019, pp. 143604; DOI <https://doi.org/10.1016/j.apsusc.2019.143604>.
9. K. Xing, Y. Xiang, M. Jiang, D.L. Creedon, G. Akhgar, S.A. Yianni, H. Xiao, L. Ley, A. Stacey, J.C. McCallum, S. Zhuiykov, C.I. Pakes and D.-C. Qi, "MoO<sub>3</sub> induces p-type surface conductivity by surface transfer doping in diamond," *Applied Surface Science*, vol. 509, 2020, pp. 144890; DOI <https://doi.org/10.1016/j.apsusc.2019.144890>.
10. S.A.O. Russell, L. Cao, D. Qi, A. Tallaire, K.G. Crawford, A.T.S. Wee and D.A.J. Moran, "Surface transfer doping of diamond by MoO<sub>3</sub>: A combined spectroscopic and Hall measurement study," *Applied Physics Letters*, vol. 103, no. 20, 2013, pp. 202112; DOI 10.1063/1.4832455.
11. J. McGhee and V.P. Georgiev, "Simulation Study of Surface Transfer Doping of Hydrogenated Diamond by MoO<sub>3</sub> and V<sub>2</sub>O<sub>5</sub> Metal Oxides," *Micromachines*, vol. 11, no. 4, 2020, pp. 433.
12. C. Verona, F. Arciprete, M. Foffi, E. Limiti, M. Marinelli, E. Placidi, G. Prestopino and G. Verona Rinati, "Influence of surface crystal-orientation on transfer doping of V<sub>2</sub>O<sub>5</sub>/H-terminated diamond," *Applied Physics Letters*, vol. 112, no. 18, 2018, pp. 181602; DOI 10.1063/1.5027198.
13. A.T. (2017.2), "Atomistix ToolKit (2017.2)," *Book Atomistix ToolKit (2017.2)*, Series Atomistix ToolKit (2017.2), ed., Editor ed.^eds., pp.
14. L.G. Ferreira, M. Marques and L.K. Teles, "Slater half-occupation technique revisited: the LDA-1/2 and GGA-1/2 approaches for atomic ionization energies and band gaps in semiconductors," *AIP Advances*, vol. 1, no. 3, 2011, pp. 032119; DOI 10.1063/1.3624562.
15. S. Smidstrup, T. Markussen, P. Vancaeyveld, J. Wellendorff, J. Schneider, T. Gunst, B. Verstichel, D. Stradi, P.A. Khomyakov, U.G. Vej-Hansen, M.E. Lee, S.T. Chill, F. Rasmussen, G. Penazzi, F. Corsetti, A. Ojanpera, K. Jensen, M.L.N. Palsgaard, U. Martinez, A. Blom, M. Brandbyge and K. Stokbro, "QuantumATK: an integrated platform of electronic and atomic-scale modelling tools," *J Phys Condens Matter*, vol. 32, no. 1, 2020, pp. 015901; DOI 10.1088/1361-648X/ab4007.
16. S. K. C, R.C. Longo, R. Addou, R.M. Wallace and K. Cho, "Electronic properties of MoS<sub>2</sub>/MoO<sub>x</sub> interfaces: Implications in Tunnel Field Effect Transistors and Hole Contacts," *Scientific Reports*, vol. 6, no. 1, 2016, pp. 33562; DOI 10.1038/srep33562.
17. H.R. Philipp and E.A. Taft, "Optical Properties of Diamond in the Vacuum Ultraviolet," *Physical Review*, vol. 127, no. 1, 1962, pp. 159-161; DOI 10.1103/PhysRev.127.159.